WASHINGTON UNIVERSITY

Department of Earth and Planetary Sciences

LOCALIZED AND WIDESPREAD CONVECTION IN THE VENUSIAN CRUST

by

Diana Leigh Goeller

A theses presented to the
Department of Earth and Planetary Sciences
of Washington University in
partial fulfillment of the
requirements for the
degree of Bachelor of Arts with Honors.

May 2013

St. Louis, Missouri

Acknowledgments. I would like to thank Washington University in St. Louis for granting me the opportunity to be evaluated for Honors with the completion of this thesis. I would also like to thank the Department of Earth and Planetary Sciences for supporting me throughout this project, most especially Dr. Phillip Skemer and Ms. Margo Mueller for their invaluable assistance with logistical details. I extend my highest gratitude to my thesis committee, Profs. V. Slava Solomatov, Doug Wiens, and Michael Wysession, who supported me even when time was less than short. Finally, I thank Dr. Solomatov especially for bringing me to this project and advising me with patience and kindness throughout.

Contents

List of Figures

List of Tables

Abstract

Two-dimensional numerical simulations of infinite Prandtl number convection in temperature-dependent viscosity fluids reflecting a range of Arrhenius rheologies applicable to the Venusian crust demonstrate the possibility of both localized (subcritical) and widespread (sub- or supercritical) convection for grain sizes within the expected range. This finding is in stark contrast with previous assumptions that the extremely dry Venusian crust does not convect. Stable localized and widespread convection are simulated in regions of mild to extreme lithospheric thinning and crustal thickening. Crustal convection may play a role in the formation of some observed surface features such as coronae. Additionally, localized and physically constrained widespread convection may help planetary scientists to understand the formation and longevity of localized planetary features, including the crustal dichotomy and Tharsis region of Mars and the asymmetric pattern of volcanism on Mercury, and may offer a mechanism for localized subduction and plate tectonics on Venus or elsewhere.

1 Introduction

Localized subcritical convection, as reported by *Solomatov* (2012), is a new tool for planetary scientists to understand enigmatic alien topography from asymmetric distributions to localized subduction and plate tectonics. While localized structures have been observed in a variety of other dynamical systems far from equilibrium − for example, in nonlinear optics and magnetoconvection (*Thual and Fauve*, 1988; *van Saarloos and Hohenberg*, 1992; *Dawes*, 2010; *Purwins et al.*, 2010) − localization in purely thermally-driven convection as proposed by *Solomatov* (2012) was not previously observed. Applied to planetary science, the existence of stable, localized convection in temperature-dependent viscosity fluids may provide answers to many long-standing questions regarding unusual gravity and topography data from terrestrial bodies.

One such body with a cornucopia of puzzling features is Venus, Earth's twin in size and

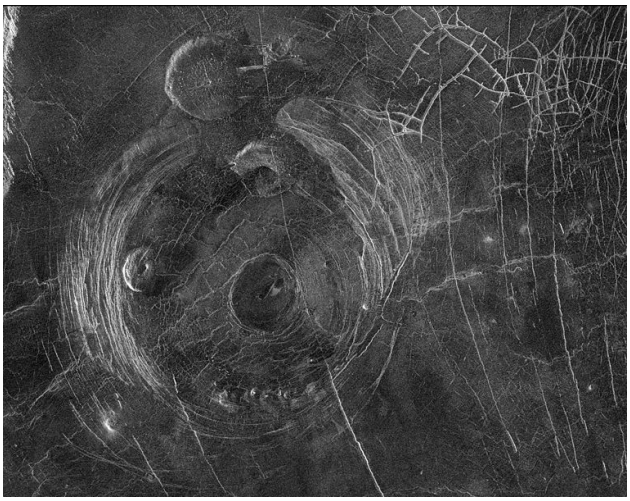

Figure 1: The Fotla Corona, approximately 300 km in diameter. Radar image obtained January 1991 by Magellan spacecraft.

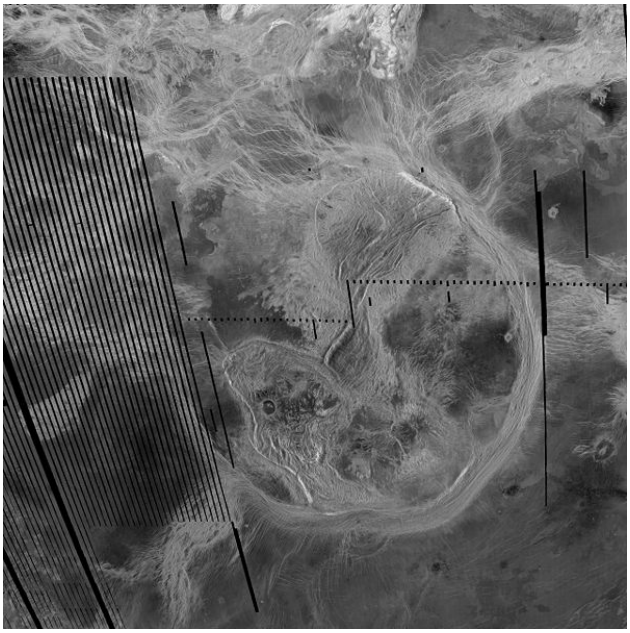

Figure 2: The Artemis Corona, nearly 2100 km in diameter, is the largest corona on the Venusian surface. Radar image obtained January 1991 by Magellan spacecraft.

little else. As an example, surface features called coronae freckle its surface in a range of sizes from 60 km in diameter to nearly 2100 km across (Figures 1 and 2). Previous studies propose a variety of mechanisms for the formation of these features, but all are based on mantle dynamic processes (*Janes et al.*, 1992; *Squyres et al.*, 1992; *Stofan et al.*, 1992, 1997; *Head et al.*, 1992; *Koch and Manga*, 1996; *Hansen*, 2003; *Johnson and Richards*, 2003; *Grindrod and Hoogenboom*, 2006; *Dombard et al.*, 2007). In contrast, we propose localized subcritical convection within the crust as another viable mechanism for the formation of coronae and other topographic features. Larger features may result from similar processes on a larger spatial scale or over a longer duration (*Stofan et al.*, 1997), which may be accounted for by steady state clusters of localized plumes or physically constrained widespread convection.

2 Localized Subcritical Convection

In fluid mechanics, the Rayleigh number (Ra) is the dimensionless ratio of buoyancy forces − the forces that drive natural convection − to viscous forces − the friction-like forces that inhibit it. The critical Rayleigh number (Ra_{cr}) is the threshold above which infinitesimal thermal perturbations induce natural thermal convection. If a finite thermal perturbation is applied to a system, however, there is a narrow range of sub-critical Ra values for which stable (non-decaying) convection may still occur in temperature-dependent viscosity fluids (*Stengel et al.*, 1982; *Richter et al.*, 1983; *White*, 1988; *Bottaro et al.*, 1992; *Capone and Gentile*, 1994; *Alikina and Tarunin*, 2000; *Solomatov and Barr*, 2006, 2008). The Ra value below which all convection eventually decays has been termed the absolute critical Rayleigh number (*Solomatov and Barr* 2006, 2008) and is denoted Ra^*_{cr}.

Though most examples that come readily to mind of thermal convection, including the churning of Earth's mantle, are high Ra flows, the study of low Ra (near Ra_{cr}) convection is important in planetary science for the study of smaller planetary bodies, including several icy satellites (*McKinnon*, 1999; *Barr and Pappalardo*, 2005; *Barr and McKinnon*, 2007; *Mitri*

and Showman, 2008) and Mercury (*Redmond and King*, 2007; *King*, 2008). Even in larger planetary bodies where high Ra convection is or may be present, low Ra flow may describe convection in other regions with lower Ra values. Between its high surface temperatures and evidence for extensive volcanic degassing, the Venusian lithosphere is assumed to be very dry, making it highly rigid and significantly lowering its Ra value (*Mackwell et al.*, 1998), but most models of the Venusian interior incorporate regular mantle plumes, which would provide sufficient thermal perturbation to initiate subcritical convection if $Ra^*_{cr} < Ra < Ra_{cr}$. Therefore, a model for convection in this setting must allow for a subcritical case.

Figure 3 shows the bifurcation diagrams of fluids with constant (top), temperature-dependent (middle), and power-law (bottom) viscosities as a function of Ra. The Nusselt number (Nu) on the vertical axis is the dimensionless ratio of convective to conductive heat flow, with $Nu = 1$ corresponding to a conductive regime and higher values corresponding to increasingly convective flow. When rocks flow - under extreme temperature and pressure conditions either within a planetary body or simulated in a laboratory - they are shown to behave with temperature-dependent viscosity (*Karato et al.*, 1986; *Karato and Wu*, 1993), so we are primarily interested in the second case. We note the narrow window of stable subcritical solutions denoted by the thick solid line in 3b, between Ra^*_{cr} and Ra_{cr}. In contrast, subcritical convection is not possible in the case of a constant viscosity fluid, and all solutions of power-law viscosity fluids are subcritical. This may become significant in future studies using a more complicated rheology than considered in this preliminary investigation.

Subcritical convection in temperature-dependent viscosity fluids has been predicted and described theoretically (*Segel and Stuart*, 1962; *Busse*, 1967; *Alikina and Tarunin*, 2000), observed in laboratory experiments (*Stengel et al.*, 1982; *Richter et al.*, 1983; *White*, 1988), and studied numerically (*Alikina and Tarunin*, 2000; *Solomatov and Barr*, 2006, 2008) with a variety of planforms. A convecting fluid's planform shows its distribution of hot rising regions and cold sinking regions within the fluid body. *Solomatov and Barr* (2006, 2008) showed planform-dependent stability in the subcritical regime, allowing for only approximate

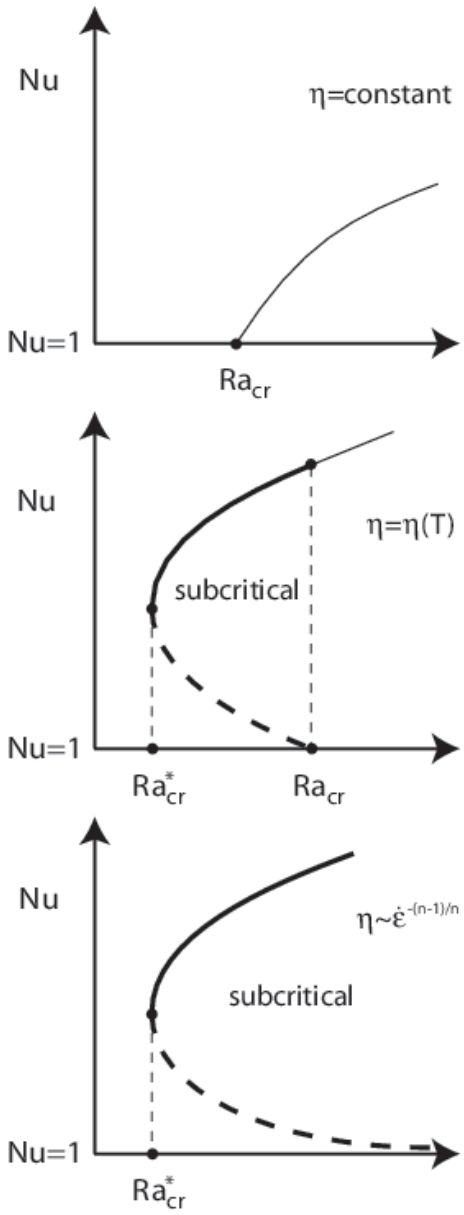

Figure 3: The bifurcation diagrams for fluids with constant (top), temperature-dependent (middle), and power-law (right) viscosities in $Ra - Nu$ axes. Ra_{cr} is the critical Rayleigh number as predicted by linear theory. At $Ra > Ra_{cr}$, conductive solutions are unstable to infinitesimal thermal perturbations and reach a solution located on the thin solid curve. This is where convection becomes widespread. At $Ra^*_{cr} < Ra < Ra_{cr}$, where Ra^*_{cr} is the absolute critical Rayleigh number, conduction is stable under infinitesimal perturbations but unstable to finite amplitude perturbations. These are the stable subcritical solutions located on the thick solid line. At $Ra < Ra^*_{cr}$, all convective motions eventually decay. The dashed line shows the locations of unstable steady-state subcritical solutions. (*Solomatov*, 2012).

values of Ra^*_{cr}.

Solomatov (2012) proposed a new type of planform only stable in the subcritical regime: a single, localized plume. In contrast to the widespread convection observed in supercritical convection, wherein any one convective cell engenders others around it with spacing on the order of the layer thickness, *Solomatov* (2012) found that a single or small cluster of convective plumes generated by a finite, localized thermal perturbation in the subcritical regime may remain spatially localized without decaying or becoming widespread.

Applied to planetary bodies, localized subcritical convection may play a role in the origin of asymmetric distributions, localization and longevity of volcanism, localized topographic rises, and peculiar regional tectonics on some planetary bodies. In particular, we propose that localized convection may exist within the Venusian crust, causing or aiding the formation of certain features. This study focuses on the first part of this hypothesis, assessing the feasibility of Venusian crustal convection using a two-dimensional finite element numerical model. Unlike the simplified exponential viscosity law used by *Solomatov* (2012), we use a more realistic Arrhenius viscosity function with parameters constrained by laboratory experiments on rocks relevant to the Venusian crust.

3 Model

The finite element code CITCOM (*Moresi and Solomatov*, 1995) is used to simulate thermal convection in a two-dimensional box of depth d and width w. In all cases, the upper and lower boundaries are maintained at constant temperature, the lateral boundaries are thermally insulated, and all boundaries are set to have free-slip conditions.

3.1 Equations of Flow

The dimensionless equations for flow on which the model operates, derived from the Navier-Stokes equations assuming incompressible, infinite Prandtl number flow by diffusion creep

alone and negligible heat generation within the crust compared to the heat flux from the mantle are

$$\nabla \cdot \mathbf{u} = 0 \tag{1}$$

$$T_t + \mathbf{u} \cdot \nabla T = \nabla^2 T \tag{2}$$

$$0 = -\nabla P + RaT\mathbf{n} + \nabla \cdot [\eta(\nabla \mathbf{u} + \{\nabla \mathbf{u}\}^T)] \tag{3}$$

where $\mathbf{u}$ is the velocity vector, T is temperature, P is pressure in excess of the hydrostatic pressure, $\mathbf{n}$ is a unit vector in the z-direction, and $\eta = \eta(T)$ is the temperature-dependent viscosity. The equations are non-dimensionalized using the cell depth d for the length scale, the diffusion time κ/d^2 for the time scale, the thermal contrast $\Delta T = T_b - T_s$ within the crust assuming a linear thermal gradient for the temperature scale, a reference viscosity η_0 taken to be that at the bottom of the crust, and the quantity $\kappa/(\eta_0 d^2)$ for the pressure scale. For completeness, the full derivations of these equations appear in the appendix.

The Rayleigh number is

$$Ra \equiv \frac{\rho g \alpha \Delta T d^3}{\eta_0 \kappa}. \tag{4}$$

where ρ is the density, g the acceleration due to gravity, α the coefficient of thermal expansion, κ the thermal diffusivity, and η_0 the reference viscosity. In this study, we take η_0 to be the viscosity at the bottom of the crust because this is where conditions are most conducive to flow.

3.2 Viscosity

At steady state, the strain rate of rocks depends on temperature (T), pressure (P), grain size (h), and shear stress (σ) according to

$$\dot{\epsilon} = C \left(\frac{\sigma}{\mu}\right)^n \left(\frac{l}{h}\right)^m \exp\left(-\frac{Q^*}{RT}\right) \tag{5}$$

(*Karato and Wu*, 1993) where C is the pre-exponential factor, μ is the shear modulus, n is the stress exponent, l is the length of the Burgers vector (a description of dislocation distortion in a crystal lattice), m is the grain size exponent, $Q^* = E^* + PV^*$ is the activation enthalpy of the material, E^* is the activation energy, V^* is the activation volume, and R is the ideal gas constant. In this paper, we drop the PV^* term because it is relatively small compared to the activation energy E^* in the crust. The viscosity η related to the strain rate $\dot{\epsilon}$ according to

$$\eta = \frac{\sigma}{3\dot{\epsilon}} \tag{6}$$

(*Ranalli*, 1995). In the case of diffusion creep, which we assume predominates over dislocation creep for small perturbations, we take $n = 1$ which gives the temperature-dependent but stress-independent Arrhenius viscosity

$$\eta = \frac{\mu}{3C} \left(\frac{h}{l}\right)^m \exp\left(\frac{E^*}{RT}\right) \tag{7}$$

and the reference viscosity η_0 is taken to be the value when $T = T_b$.

In dimensionless form,

$$\eta = B_0 \exp\left(\frac{A}{T_0 + \widetilde{T}}\right) \tag{8}$$

where

$$B_0 = \exp\left(\frac{A}{T_0 + 1}\right), \qquad A = \frac{E^*}{R\Delta T}, \qquad T_0 = \frac{T_s}{\Delta T}$$

and

$$\widetilde{T} = \frac{T - T_s}{\Delta T}$$

ranges from $\widetilde{T}_s = 0$ at the surface to $\widetilde{T}_b = 1$ at the base of the crust. A more lengthy derivation of these values and expressions appears in the appendix.

3.3 The Perturbation

To generate spatially localized convection, the initial thermal perturbation must be localized (*Solomatov*, 2012). In a terrestrial body, this may arise from a mantle plume in a deeper layer (e.g. *Courtillot et al.*, 2003). Following *Solomatov* (2012), we use a simple Gaussian distribution, the dimensionless, two-dimensional form of which is

$$T(x, z) = T_{cond}(z) + \delta T(x, z) \tag{9}$$

where $T_{cond}(z) = z$ is the conductive temperature profile in dimensional form and

$$\delta T(x, z) = \delta T_0 e^{-r^2/r_0^2} \cos(kx) \sin(\pi z) \tag{10}$$

is the perturbation function, δT_0 is the perturbation amplitude, k is the wavenumber of the perturbation, and r is the Euclidian distance between some origin point x_0 and the point x. The scaling parameter r_0 controls the width of the perturbed region. The appendix includes a short discussion on the non-dimensionalization of this equation.

For numerical reasons, small harmonic perturbations are also added through the entire region, though their amplitude is chosen to be sufficiently small ($< 1\%$) so that they decay with time and are not responsible for widespread convection.

In all trial runs in this study, the perturbation was centered at the middle of a 192×32 finite element grid (dimensionless height $d = 1$ and width $w = 6$). *Solomatov* (2012) demonstrated that higher resolution affected results by less than $\sim 1\%$. In the perturbation, we let $\delta T_0 = 0.3$, $r_0 = 0.5$, and the wavenumber $k = 2\pi$.

4 Choice of Model Parameters

The parameter values used in this study appear in Table 1 (*Karato and Wu*, 1993; *Solomatov and Moresi*, 1996; *Rybacki and Dresen*, 2000; *Hirth and Kohlstedt*, 2003; *Korenaga and Karato*, 2008; *Orth and Solomatov*, 2012). As is apparent from the table, some of the values are well-established while other remain highly uncertain. The values for C, E, and m are derived experimentally for a given material and depend on the fugacity (water content) of the material and the primary mechanism of flow. In this study, we take values derived from dry samples deformed in the diffusion creep regime. The temperature contrast $\Delta T = T_b - T_s$ between the bottom and top of the crust is derived assuming a linear thermal gradient throughout the lithosphere, the base of which we assume has a constant temperature around $T_i = 1730$ K (*Orth and Solomatov*, 2012); for simplicity, we assume $T_i - T_s = 1000$ K. The range of values for crust thickness is as proposed in *Orth and Solomatov* (2012), and the values used for lithosphere thickness are consistent with present-day estimates of thin to average lithosphere (*McKenzie*, 1994; *Kucinskas and Turcotte*, 1994; *Phillips*, 1994; *Smrekar*, 1994; *Solomatov and Moresi*, 1996; *Nimmo and McKenzie*, 1996, 1998; *Moore and Schubert*, 1997; *Simmons, et al.*, 1997; *Vezolainen, et al.*, 2004; *Reese, et al., 2007*; *Orth and Solomatov*, 2012).

4.1 Rheological Law

The rheology of a material can be summarized by the relationship between stress (σ) and strain rate ($\dot{\epsilon}$), as in equation (5), reproduced below.

$$\dot{\epsilon} = C \left(\frac{\sigma}{\mu}\right)^n \left(\frac{l}{h}\right)^m \exp\left(-\frac{Q}{RT}\right)$$

This relationship is known as the rheological law or flow law, and it is highly dependent on the material and the conditions under which it is deformed. Under low stress, as we assume in this study, diffusion creep predominates over dislocation creep so that the relationship

Table 1: Parameter values

Parameter	Notation	Value
Shear modulus	μ	80 GPa
Pre-exponential factor	C	$8.7 \times 10^{15} - 8.1 \times 10^{26}$ s^{-1}
Grain size	h	$0.01 - 1$ cm
Length of Burgers vector	l	0.5 nm
Grain size exponent	m	$2.5 - 3$
Activation energy	E^*	$261 - 375$ kJ mol^{-1}
Universal gas constant	R	8.31 J mol^{-1} K^{-1}
Crust thickness	d	$40 - 80$ km
Lithosphere thickness	D	$100 - 300$ km
Surface temperature	T_s	733 K
Interior temperature	T_i	1733 K
Crust thermal contrast	ΔT	$130 - 800$ K
Crust density	ρ_0	3300 kg m^{-3}
Acceleration due to gravity	g	8.9 m s^{-2}
Thermal diffusivity	κ	8.1×10^{-7} m^2 s^{-1}
Coefficient of thermal expansion	$\bar{\alpha}$	3×10^{-5} K^{-1}

between stress and strain is linear and we take $n = 1$. At higher stresses, dislocation creep will induce a higher stress exponent. Rheological studies report values for Q (or E^* in cases like ours where the PV^* term is considered negligibly small in comparison), m, and C in the diffusion and dislocation creep regimes separately.

Water can also greatly enhance a material's susceptibility to flow, so separate rheological laws are also developed for wet and dry samples of a material. The definitions of "wet" and "dry" may vary slightly between studies, and it is important to check the applicability of a given study. For example, "dry" samples in *Shelton and Tullis* (1981) were removed of adsorbed water, but hydrous minerals were left to release their water during deformation, while *Karato and Wu* (1993) used only water-free dry samples. Between its high surface temperatures and evidence for extensive volcanic degassing, Venus is assumed to have an extremely dry lithosphere (*Mackwell et al.*, 1998), so the dry laws produced by the latter study are more appropriate for Venus. Likewise, the "dry" condition in *Hirth and Kohlstedt*, (2003) and *Korenaga and Karato*, (2008) referred to samples that were anhydrous to the detection limit of Fourier transformation infrared spectroscopy (FTIR).

These three studies - *Karato and Wu* (1993), *Hirth and Kohlstedt* (2003), and *Korenaga and Karato* (2008) - used olivine as the deforming material. Olivine is assumed to be the material governing the rheology of the Earth's upper mantle, since it is its weakest major phase (*Korenaga and Karato*, 2008). In recent studies, olivine has also been used as a proxy for Venusian rheology (e.g. *Vezolainen, et al.*, 2004; *Reese, et al.*, 2007), and we follow this lead. While little data exists to support or undermine this decision, we find it beneficial to additionally consider a flow law for a material more similar in composition to the Venusian surface. To be clear, rheology is not a function of composition *per se*, but the mineral that will dominate a material's rheology will be one of its major constituents. In any case, this will give us a sense for the uncertainties associated with rheological law in our estimates of convection in the Venusian crust.

Measurements by the Russian landers (*Surkov et al.*, 1983, 1984, 1986) indicate that the Venusian crust is primarily basaltic in composition, which may not be surprising given its extensive volcanic history. Because of this, *Mackwell et al.* (2008) conducted rheological studies on two carefully-chosen and extensively dried samples of basaltic diabase to specifically investigate the rheology of the Venusian lithosphere. Unfortunately, because their focus was the deep lithosphere, they derived flow laws in the dislocation regime only. However, *Rybacki and Dresen* (2000) derived both dislocation and diffusion creep flow laws for wet and dry samples of synthetic anorthite, another basaltic diabase. We note that "dry" samples in this study contained a small but detectable amount of water by FTIR measurement (640 ± 260 ppm H/Si or 0.004 ± 0.002 wt % H_2O), but within a wide margin of error, we assume this does not greatly affect the results.

The parameter values for the four laws used in this study are summarized in Table 2.

4.2 Lithosphere Thickness

Present estimates for Venusian lithosphere thickness are only loosely constrained. *Orth and Solomatov* (2012) were able to match gravity and topography data precisely to a wide

Table 2: Rheological Constraints

	Karato and Wu 1993	*Rybacki and Dresen* 2000	*Hirth and Kohlstedt* 2003	*Korenaga and Karato* 2008
C	8.70×10^{15} s^{-1}	8.06×10^{26} s^{-1}	9.69×10^{26} s^{-1}	1.12×10^{23} s^{-1}
E^*	300 kJ mol^{-1}	290 kJ mol^{-1}	375 kJ mol^{-1}	261 kJ mol^{-1}
m	2.5	3	3	2.98

range of average lithosphere thicknesses, but were able to constrain their results slightly by considering melt generation rates. As an upper bound, the lithosphere cannot have grown thicker than $\sim$ 800 km over its entire history in the absence of any other processes (*Orth and Solomatov*, 2012). Evidence for recent volcanic eruptions (*Mueller et al.*, 2008; *Smreker et al.*, 2010), indicates that the lithosphere must be thin enough, at least in some places, for melt to form and escape. Requiring lithospheric thinning to at least 300 km to meet this condition, *Orth and Solomatov* (2012) showed that any average lithosphere thickness less than 500 km for crust thicknesses ranging 40-80 km produced at least one region satisfying the constraint. At the other end, the lithosphere cannot be regionally thinner than 80 km, as this would produce too much melt (*Orth and Solomatov*, 2012).

Turcotte (1993) proposed a Venusian history including episodic plate tectonics, with a lithosphere cooled by thermal conduction over the last 500 million years to no more than 300 km. The model produced by *Orth and Solomatov* (2012) was unable to reproduce an average lithosphere thickness less than $\sim$ 300 km that precisely matched gravity and topography data without it being thinner than the crust in some places, though an earlier study using a different model predicted an average lithosphere thickness of 250 km (*Orth and Solomatov*, 2009). *Vezolainen, et al.* (2003) introduced the additional constraint of geomorphological estimates of the uplift time of Beta Regio, and results using a three-dimensional model satisfying gravity, topography, olivine rheology, and uplift time data supported a lithosphere thickness $\sim$ 400 km (*Vezolainen et al.*, 2004). *Reese et al.*, 2007 likewise found evidence for recent lithospheric thickening to present values consistent with previous estimates $\sim$ 100 km

to 400 km (*McKenzie*, 1994; *Kucinskas and Turcotte*, 1994; *Phillips*, 1994; *Smrekar*, 1994; *Solomatov and Moresi*, 1996; *Nimmo and McKenzie*, 1996, 1998; *Moore and Schubert*, 1997; *Simmons, et al.*, 1997).

In this study, we consider lithosphere and crust thicknesses dependently, beginning with conditions most conducive to flow and proceeding to less extreme cases, allowing thicker crust to correlate with lithospheric thinning.

4.3 Grain Size

Grain size varies with depth and temperature (e.g. *Karato and Wu*, 1993; *Solomatov and Reese*, 2008), and at the range of values we are considering, grain sizes are expected to be within the range of 0.1 mm to 1 cm. However, recognizing that the uncertainty of our rheological and physical parameters may significantly increase the uncertainty in grain size, we consider an extended range of conceivable grain sizes from 0.01 mm to 10 cm.

5 Results

Using the non-dimensional equations above, trials in this study are dependent only on the parameters T_0, B_0, and Ra. T_0 is a function only of the crust (d) and lithosphere (D) thicknesses, and B_0 is constant for fixed T_0 and a particular rheological law. For a given law and thermal contrast, Ra is adjusted in increments of 5×10^4 (for $\Delta T = 200 - 800$ K) or 1×10^4 (for $\Delta T = 80 - 125$ K). Results in terms of Ra can then be converted to more intuitive results in terms of grain size h since all other values on which Ra depends are assumed constant in a particular trial. Figures 4 and 5 show the range of Rayleigh numbers and grain sizes respectively for which the model produced unstable (decaying), localized, and widespread convection. Example sequences for each convective regime appear in Figures 6-9.

In Figures 4 and 5, results are grouped by the assumed rheological law and labeled according the study from which the assumed law came. The first bar in each group corresponds

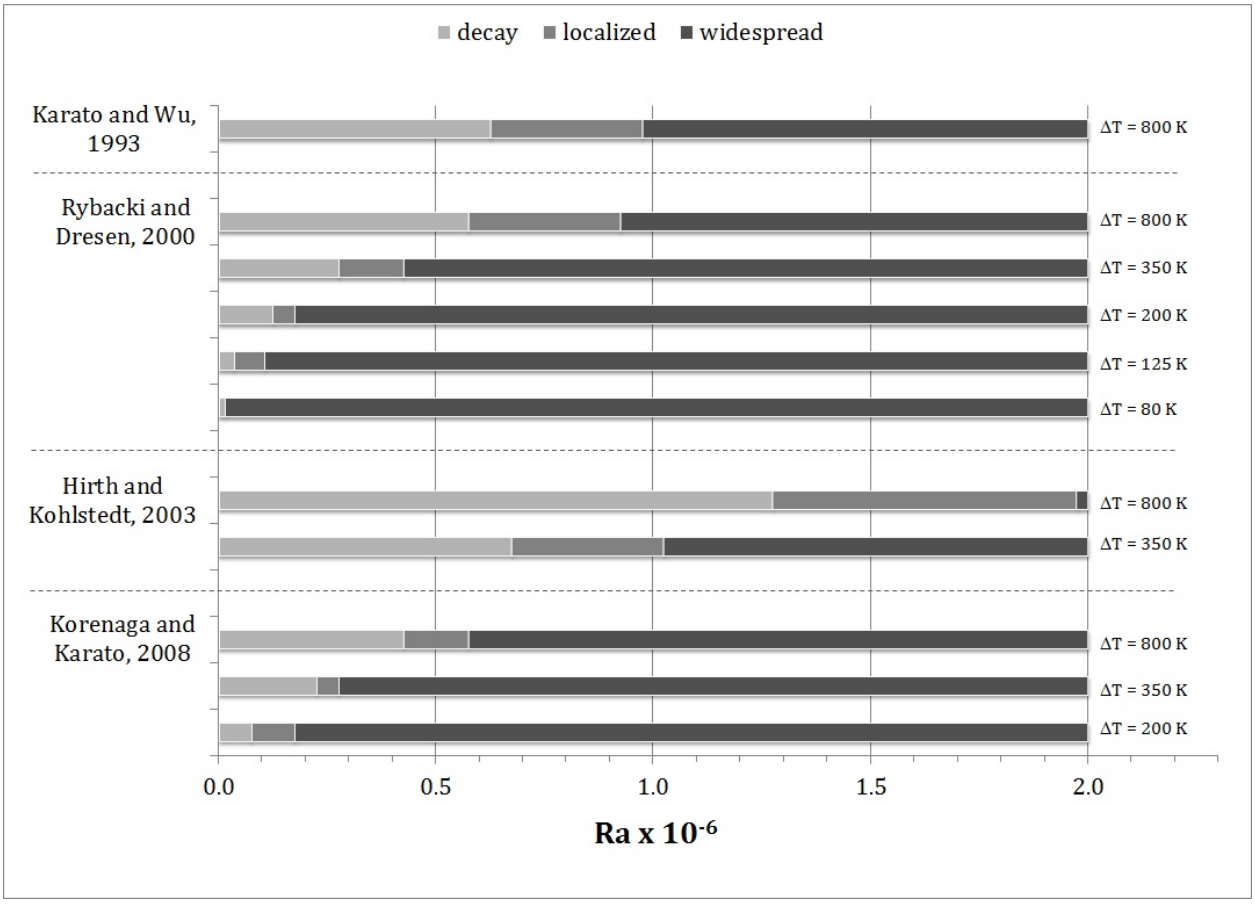

Figure 4: Model results in terms of the Rayleigh number Ra. The darkest regions correspond to solutions where convection became widespread, so $Ra > Ra_{cr}$. The middle regions correspond to stable subcritical solutions, $Ra^*_{cr} < Ra < Ra_{cr}$, in which convection remained a localized plume. The lightly shaded regions show where convection decayed, so $Ra < Ra^*_{cr}$. Trials are grouped by the rheology assumed with groups labeled by the study in which the rheological law was derived. The top bar for each rheology corresponds to trials conducted with crust thickness $d = 80$ km and lithosphere thickness $D = 100$ km. For each subsequent bar in each group, where present, d is decreased by 10 km and D is increased by 100 km. Trials are ceased for a particular rheology when convection can no longer be produced for grain sizes larger than 0.1 mm (see Figure 5). In the bottommost bar of the *Rybacki and Dresen, 2000* trials, the localized subcritical window was too narrow to be detected between the increments of $Ra = 1 \times 10^4$. Dividends between the regimes are made evenly between trial intervals of 5×10^4 for the top three bars ($\Delta T = 200 - 800$ K) and 1×10^4 for lower bars ($\Delta T = 80 - 125$ K) where present. The lower dividend is an estimate for Ra^*_{cr} and the upper an estimate for Ra_{cr}.

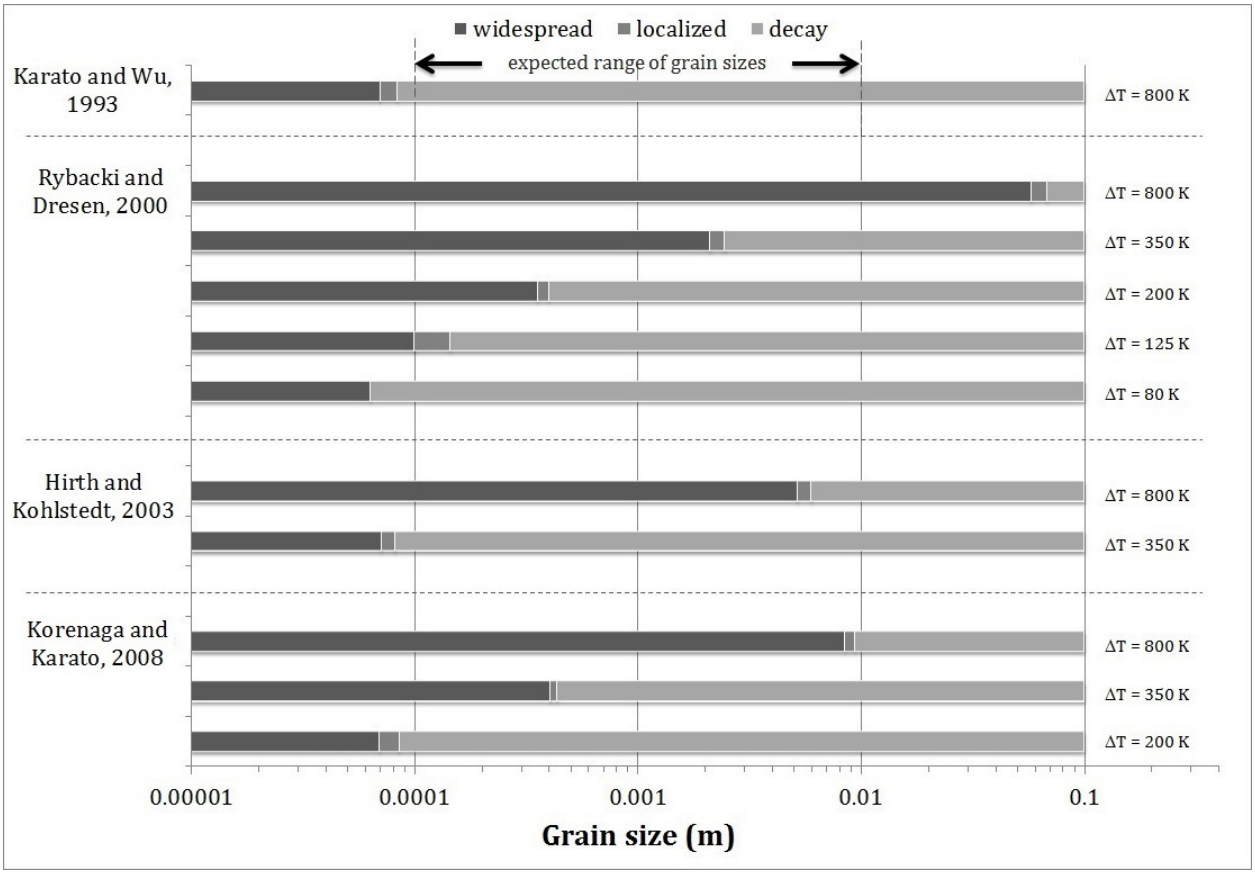

Figure 5: Model results in terms of the grain size h. The results tabulated in Figure 4 in terms of Ra are presented here in terms of the corresponding grain size h, where all other parameters on which Ra depends are assumed constant in any particular trial. Each bar corresponds to the same trials as in Figure 4. As there, the darkest regions correspond to solutions in which convection became widespread, so $Ra > Ra_{cr}$, the middle regions correspond to stable subcritical solutions, $Ra^*_{cr} < Ra < Ra_{cr}$, in which convection remained a localized plume, and the lightly shaded regions show where convection decayed, so $Ra < Ra^*_{cr}$. Trials are grouped by the rheology assumed with groups labeled by the study in which the rheological law was derived. The top bar for each rheology corresponds to trials conducted with crust thickness $d = 80$ km and lithosphere thickness $D = 100$ km. For each subsequent bar in each group, where present, d is decreased by 10 km and D is increased by 100 km. Trials are ceased for a particular rheology when convection can no longer be produced for grain sizes larger than 0.1 mm. In the bottommost bar of the *Rybacki and Dresen, 2000* trials, the localized subcritical window was too narrow to be detected between the increments of $Ra = 1 \times 10^4$. Dividends between convection regimes are made evenly between the grain sizes calculated from the Ra values on either side of Ra_{cr} or $Ra_{cr}*$.

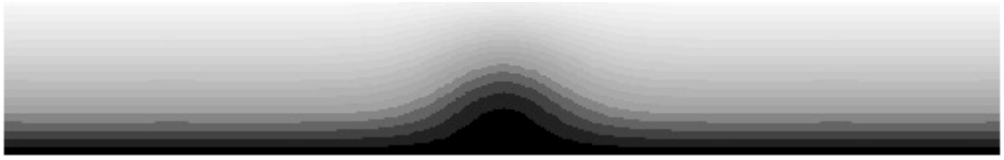

Figure 6: The temperature field generated by the initial perturbation in the 192×32 finite element grid. This is the first frame in every trial run regardless of rheological law, physical parameters, or the Rayleigh number.

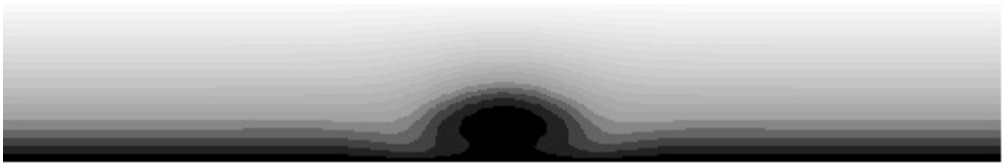

Figure 7: An example temperature field in the 192×32 finite element grid of our model in which the initial thermal perturbation induces localized subcritical convection. This plume is stable and has reached steady state. This snapshot depicts timestep 1800 of a trial conducted with the dry diffusion rheological law reported in *Hirth and Kohlstedt* (2003) assuming a crust thickness $d = 80$ km and lithosphere thickness $D = 100$ km, resulting in a temperature contrast $\Delta T = 800$ K in the crust, and Rayleigh number $Ra = 1.5 \times 10^6$.

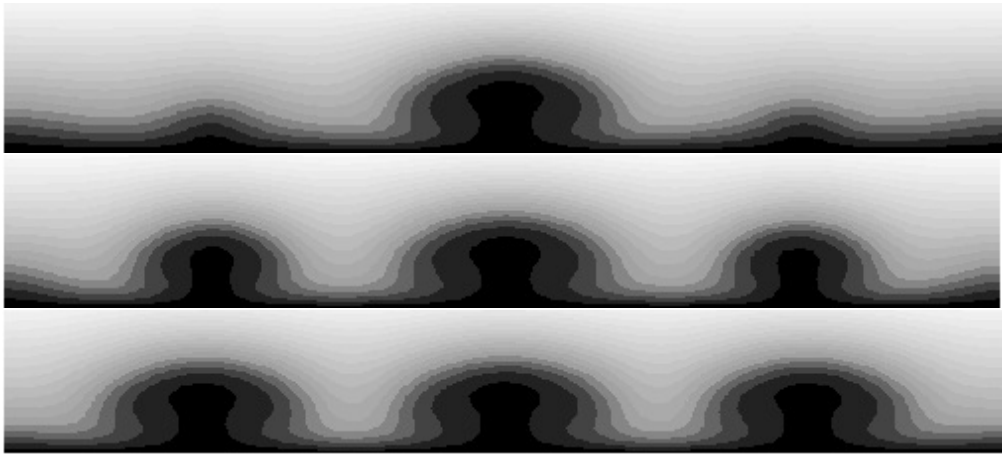

Figure 8: An example sequence of temperature fields in the 192×32 finite element grid of our model in which convection becomes widespread. These snapshots depict timesteps 400, 500, and 600 of a trial conducted with the dry diffusion rheological law reported in *Korenaga and Karato* (2008) assuming a crust thickness $d = 70$ km and lithosphere thickness $D = 200$ km, resulting in a temperature contrast $\Delta T = 350$ K in the crust, and Rayleigh number $Ra = 3.0 \times 10^5$.

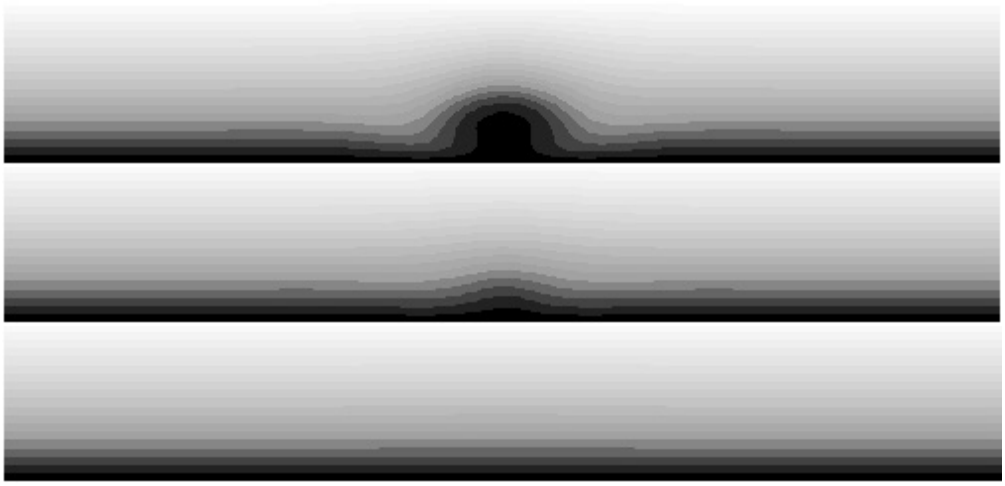

Figure 9: An example sequence of temperature fields in the 192×32 finite element grid of our model in which the initial thermal perturbation is unstable and decays. These snapshots depict timesteps 100, 300, and 500 of a trial conducted with the dry diffusion rheological law reported in *Rybacki and Dresnen* (2000) assuming a crust thickness $d = 80$ km and lithosphere thickness $D = 100$ km, resulting in a temperature contrast $\Delta T = 800$ K in the crust, and Rayleigh number $Ra = 5.5 \times 10^5$.

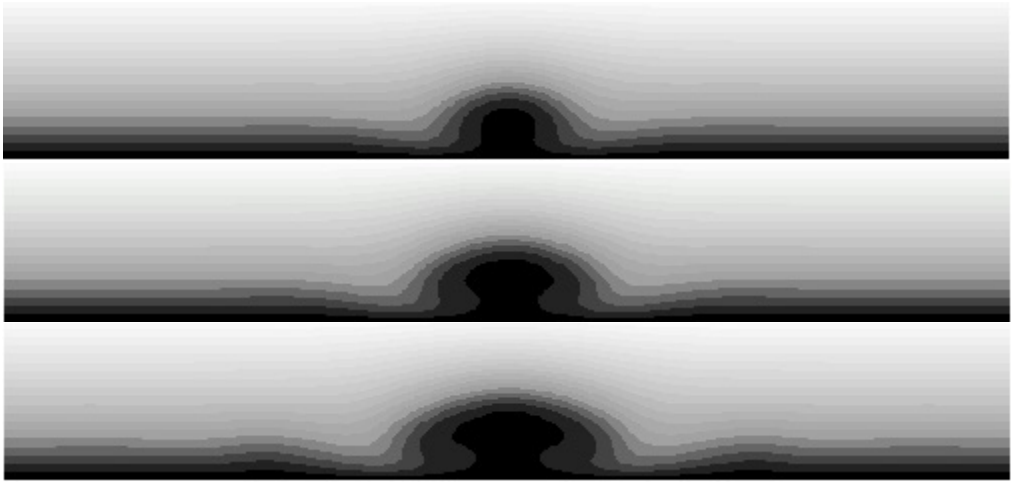

Figure 10: An example of the dependence of localized convective cell size on the Rayleigh number Ra. These snapshots depict the temperature fields of steady state localized subcritical plumes generated by the model assuming the rheological law reported in *Karato and Wu* (1993) for $Ra = 6.5 \times 10^5$ (just above the absolute critical Rayleigh number Ra^*_{cr}; top), $Ra = 8.0 \times 10^5$ (middle), and $Ra = 9.5 \times 10^5$ (just below the critical Rayleigh number Ra_{cr}; bottom).

to trials with $d = 80$ km and $D = 100$ km, resulting in a temperature contrast within the crust of $\Delta T = 800$ K. Each successive bar in a group, where present, refers to trials in which d is decreased by 10 km and D is increased by 100 km. This results in successive thermal contrasts, where present, of $\Delta T = 800$ K, 350 K, 200 K, 125 K, and 80 K, as labeled. Trials are continued until stable convection is not obtained for grain sizes within the expected range of $h = 0.1$ mm - 1 cm, as depicted in Figure 5. In the bottommost bar of the *Rybacki and Dresen, 2000* trials, the localized subcritical window was too narrow to be detected between the increments of $Ra = 1 \times 10^4$.

Where localized convection was found for a range of Ra under the same physical and rheological constraints, we observed an increase in steady state cell size with increasing Ra. Figure 10 depicts the temperature fields of steady state subcritical solutions from the trials assuming *Karato and Wu* (1993) rheology for $Ra = 6.5 \times 10^5$, (just above Ra^*_{cr}), $Ra = 8.0 \times 10^5$, and $Ra = 9.5 \times 10^5$ (just below Ra_{cr}).

6 Discussion and Conclusions

Unexpectedly, our investigation of localized convection in the Venusian crust gives way to the possibility of widespread convection under three of the four rheological laws studied. Although the crust would only support stable convection under the *Karato and Wu* (1993) rheological law in the most generous circumstances, for a thin lithosphere 100 km thick and a crust thickened to 80 km, corresponding to a temperature contrast $\Delta T = 800$ K, the other three laws produce widespread convection for nearly the full range of expected grain sizes. Both the *Rybacki and Dresen* (2000) law for anorthite and the *Korenaga and Karato* (2008) law for olivine show widespread convection for expected grain sizes with temperature contrast only $\Delta T = 350$ K, corresponding to lithosphere thickness $D = 200$ km and crust thickness $d = 70$ km. These values correspond what several models predict under many of the largest topographical features (*Anderson and Smrekar*, 2006; *Orth and Solomatov*, 2012).

The *Rybacki and Dresen* (2000) law even supports subcritical convection for expected grain sizes with thermal contrast as low as $\Delta T = 125$ K, corresponding to lithosphere thickness $D = 400$ km and crust thickness $d = 50$ km. Many studies support both of these values as close to the global average (*McKenzie*, 1994; *Kucinskas and Turcotte*, 1994; *Phillips*, 1994; *Smrekar*, 1994; *Solomatov and Moresi*, 1996; *Nimmo and McKenzie*, 1996, 1998; *Moore and Schubert*, 1997; *Simmons, et al.*, 1997; *Vezolainen, et al.*, 2004; *Reese, et al.*, 2007). In other words, both localized and widespread convection may be very real phenomena within the Venusian crust.

It should be emphasized that all of the rheological laws here considered are relatively simple and our calculations include wide margins for error. As noted before, the *Rybecki and Dresen* (2000) law was derived from samples with slightly greater water content than those in the other studies and perhaps more than is present in the Venusian crust. The composition of the Venusian crust remains unknown, and geoid and topography data support a wide range of crust and lithosphere thicknesses (*Orth and Solomatov*, 2012). Results may also be skewed by projection into two dimensions, and a three-dimensional model may show different results (e.g. *Vezolainen et al.*, 2004). Partial melt and compositional buoyancy would also affect the system dynamics and would need to be investigated. Finally, our calculations assume flow by diffusion creep only, but in the case of widespread convection this would almost certainly be invalid. Future studies should consider how the flow laws would change after the onset of convection in this regime.

Nonetheless, these results suggesting stable localized and widespread convection within the Venusian "stagnant lid" (*Solomatov and Moresi*, 1996) raise questions for future study. Not only may localized convection be responsible for a variety of surface features, including coronae and localized topographic rises, widespread convection may also play a significant role. In fact, given the narrow range of physical parameters in which subcritical convection occurs, widespread convection seems more likely to occur in the Venusian crust than subcritical convection. Physical requirements such as an above-average lithosphere thickness

may constrain widespread convection to behave much like a cluster of localized plumes, or it may pervade under wide regions with above average thermal contrasts. Stable localized convection may engender widespread convection if crust thickens or lithosphere thins over time. Widespread convection may be responsible for larger topographic features while single localized plumes may result in smaller surface expressions such as small- to medium-sized coronae (*Stofan et al.*, 1997). An investigation of the topography produced by these phenomena assuming brittle deformation of the crust may give clues to the formation of these and other surface features. The application of these models to other planets − including the Earth − may provide valuable insight into the history and dynamics of these bodies, as well.

Furthermore, it is likely that convective cells of different magnitudes produce distinguishable topography. Since localized convective cell size depends on Ra (see Figure 10), better understanding the relationship between convective cell size and the resulting topography compared with observational data may offer new insight into the rheological properties and shallow internal structure of Venus and other terrestrial bodies.

In conclusion, it is important for future studies to consider the effects that localized or widespread convection may have on a variety of terrestrial bodies − even Earth. Noting the dependence of the convective cell widths on physical and rheological parameters, observations of convection-generated topography may provide a new tool for studying their shallow internal structure if convective cell width has an effect on observable topography. Additionally, these processes could play a major role in the origin of many unsolved problems in planetary science (see *Solomatov*, 2012). These include asymmetric distributions, as of volcanism on Mercury (*Roberts and Barnouin*, 2012); localization and longevity of volcanism on Venus or the early dynamo of the Moon (*Stegman et al.*, 2003); localized topographic rises, such as the Atla and Beta Regio of Venus (*Vezolianen et al.*, 2004) or the crustal dichotomy and Tharsis on Mars (*Harder and Christensen*, 1996; *Zhong and Zuber*, 2001; *Reese et al.*, 2011; *Wenzel et al.*, 2004; *Ke and Solomatov*, 2006; *Reese et al.*, 2007; *Zhong*, 2008); and peculiar regional tectonics on Venus or other planetary bodies. Considering the problem of subduction ini-

tiation and the onset of plate tectonics (*Fowler*, 1993; *Trompert and Hansen*, 1998; *Moresi and Solomatov*, 1998; *Bercovici*, 2003; *Valencia et al.*, 2007; *O'Neill et al.*, 2007; *Korenaga*, 2010; *van Heck and Tackley*, 2011), localized or physically constrained widespread convection within the crust may offer a mechanism for localized subduction and plate tectonics, which was proposed on Venus nearly two decades ago (*Sandwell and Schubert*, 1995). We hope all these avenues are pursued in future work.

A Appendix: Derivations

The following derivations are included for completeness and a fuller understanding of the origin of the equations on which the model used in this study was based.

A.1 Navier-Stokes Equations

The Navier-Stokes equations provide the basis for everything in fluid mechanics. They express the fundamental concepts of the conservation of mass, energy, and momentum, and together can describe the precise movement of any fluid with known properties obeying Newtonian mechanics. However, exact solutions can only be found for rare cases that do not occur in rock mechanics. Fortunately, given such an application as rock mechanics, many simplifications may be made without compromising accuracy, since some terms are so small compared to others that they may be neglected for the given type of flow. In this section, we derive the equations that govern the flow of planetary interiors.

We also non-dimensionalize the equations. Non-dimensionalization is an important mathematical tool that allows us to analyze systems independent of scale. Equations are non-dimensionalized by relating every parameter to characteristics of the system. In other words, only relative magnitudes matter, and systems with the same relations produce identical behavior, regardless of the actual sizes of either system. Hence, a numerical box of 192×32 finite elements can well approximate a portion of the Venusian crust 80 km thick.

The three Navier-Stokes equations, in their raw form, are the following:

$$\frac{\partial \rho}{\partial t} + \frac{\partial}{\partial x_i}(\rho u_i) = 0 \tag{A.1}$$

$$\rho T \frac{Ds}{Dt} = \tau_{ij} \frac{\partial u_i}{\partial x_i} + \frac{\partial q_i}{\partial x_i} + \rho H \tag{A.2}$$

$$\rho \frac{Du_i}{Dt} = -\frac{\partial P}{\partial x_i} + \frac{\partial \tau_{ij}}{\partial x_j} + \rho g_i \tag{A.3}$$

where ρ is density, u is velocity and each x_i is an orthogonal Cartesian spatial direction, T

is temperature, s is entropy, τ_{ij} is the stress tensor, q is the heat flux vector, H is the rate of internal heat generation per unit mass, P is pressure, g is gravity, and the operator

$$\frac{D}{Dt} = \frac{\partial}{\partial t} + u_i \frac{\partial}{\partial x_i} \tag{A.4}$$

is the total derivative. Equation (A.1) is the equation for conservation of mass, (A.2) conservation of energy, and (A.3) conservation of momentum.

A.1.1 Conservation of Mass

To simplify equation (A.1), let us first expand the second term,

$$\frac{\delta(\rho u_i)}{\delta x_i} = \rho \frac{\partial u_i}{\partial x_i} + u_i \frac{\partial \rho}{\partial x_i}. \tag{A.5}$$

We now employ the Boussinesq approximation, which is standard procedure in rock mechanics. First, we assume that our fluid (the Venusian crust) behaves as an incompressible fluid, so density is spatially constant ($\partial\rho/\partial x_i = 0$). Additionally, we assume that the relative change in density over time as warmed material rises and cooled material sinks is also small enough to be disregarded ($\partial\rho/\partial t = 0$). Thus, we neglect density variation entirely, except as it relates to the buoyancy force in the conservation of momentum equation. Dividing by density, this leaves us with only

$$\frac{\partial u_i}{\partial x_i} = 0. \tag{A.6}$$

To non-dimensionalize this equation, we introduce the cell depth d as a characteristic length and the diffusion time d^2/κ as a characteristic time, where κ is the thermal diffusivity. Together, they produce a characteristic viscosity $u_0 = \kappa/d$. Returning to equation (A.6) we derive:

$$\begin{aligned}\frac{\partial u_i}{\partial x_i} &= \frac{\partial u_i \cdot \frac{u_0}{u_0}}{\partial x_i \cdot \frac{d}{d}} \\ &= \frac{\partial \frac{u_i}{u_0} \cdot u_0}{\partial \frac{x_i}{d} \cdot d} \\ &= \left(\frac{u_0}{d}\right) \frac{\partial \widetilde{u_i}}{\partial \widetilde{x_i}} = 0\end{aligned} \tag{A.7}$$

where the $\sim$ is introduced to denote dimensionless parameters, though we will drop it for neatness where there is no ambiguity. After dividing by the constants, we see that the non-dimensional form of equation (A.6) looks the same as the dimensional form, except that the parameters are dimensionless.

In equations 1 - 3 in the main body of the text, a compact notation is introduced using the gradient operator,

$$\nabla = \left(\frac{\partial}{\partial x} + \frac{\partial}{\partial y} + \frac{\partial}{\partial z}\right) \tag{A.8}$$

in which the last line of equation A.7 becomes

$$\nabla \cdot \mathbf{u} = 0$$

where $\mathbf{u}$ is the velocity vector.

A.1.2 Conservation of Energy

Turning our attention to the conservation of energy, equation (A.2), we have

$$\rho T \frac{Ds}{Dt} = \tau_{ij} \frac{\partial u_i}{\partial x_i} + \frac{\partial q_i}{\partial x_i} + \rho H$$

(restated from above). To simplify, we first assume that the heat generated within the crust ρH is small compared to the other terms and neglect it. This assumption is justified since most of the decaying radioactive isotopes that generate heat are heavier materials concentrated in the core and mantle of the planet.

Next we introduce another standard approximation in rock mechanics: that of the effectively infinite Prandtl number Pr or low Reynolds number Re_d, which just means that flow occurs very slowly (we will consider these a little more closely in manipulating the conservation of momentum equation next). Through dimensional manipulation similar to the non-dimensionalization procedure above, it can be shown that the first term on the right side of equation (A.2) scales with Re_d or inversely with Pr, and so is small enough compared to the other terms to be neglected.

In fluid mechanics, low Reynolds number flow is often called "creeping flow," and in rock mechanics flow is generally described as a combination of diffusion creep and dislocation creep. At the onset of convection in rock materials, as in the case of subcritical convection following a thermal perturbation, flow occurs predominantly if not only by diffusion creep. Diffusion creep continues to dominate in conditions of relatively low stress, small grain size, low temperature, and high pressure (*Karato and Wu*, 1993). Since we can expect that Venusian crustal material is subject to most of these conditions, we make the simplifying assumption that flow occurs only by diffusion creep within the Venusian crust. It follows from this that the deformed minerals assume an isotropic distribution (*Karato and Wu*, 1993), allowing us to use Fourier's law of heat conduction to make the following substitution:

$$q_i = -k\frac{\partial T}{\partial x_i} \tag{A.9}$$

where k is thermal conductivity. Assuming a roughly homogeneous crust, we take k to be constant and pull it outside the outer derivative in equation A.2.

Finally, we employ thermodynamic identities to replace the term on the left side of equation (A.2) with

$$\rho T\frac{Ds}{Dt} = \rho c_p\frac{DT}{Dt} - \alpha T\frac{D\rho}{Dt} \tag{A.10}$$

where c_p is specific heat capacity and α is the coefficient of thermal expansion or thermal

expansivity (*Schubert et al.*, 2001). By the Boussinesq approximation, we can again ignore the variation in density and so drop the second term, so we have

$$\rho c_p \frac{DT}{Dt} = k \frac{\partial^2 T}{\partial x_i^2} \tag{A.11}$$

and dividing both sides by k, we get

$$\frac{1}{\kappa} \frac{DT}{Dt} = \frac{\partial^2 T}{\partial x_i^2} \tag{A.12}$$

where $\kappa \equiv k/(\rho c_p)$ is the thermal diffusivity as previously introduced. This is the simplified form of the equation for conservation of energy.

We can non-dimensionalize this equation following the same procedure as used above with the equation for conservation of mass. We introduce the parameters T_s, the constant temperature at the top of our fluid layer (the Venusian surface), and T_b, the constant temperature at the bottom of the fluid layer (the base of the Venusian crust), and define the thermal contrast $\Delta T = T_b - T_s$. We will use ΔT for the temperature scale, and specific temperature values will be computed non-dimensionally as

$$\widetilde{T} = \frac{T - T_s}{T_b - T_s} \tag{A.13}$$

so that we get the boundary conditions $\widetilde{T}_s = 0$ at the surface and $\widetilde{T}_b = 1$ at the base of the fluid layer.

Expanding the total derivative, we derive:

$$\frac{1}{\kappa} \cdot \left(\frac{\Delta T \kappa}{d^2} \right) \cdot \left[\frac{\partial \widetilde{T}}{\partial \widetilde{t}} + \widetilde{u}_i \cdot \frac{\partial \widetilde{T}}{\partial \widetilde{x}_i} \right] = \left(\frac{\Delta T}{d^2} \right) \cdot \frac{\partial^2 \widetilde{T}}{\partial \widetilde{x}_i^{\,2}} \tag{A.14}$$

from which we immediately see that the constants cancel and we are left with a simplified, dimensionless form of the equation for the conservation of energy:

$$\frac{\partial T}{\partial t} + u_i \cdot \frac{\partial T}{\partial x_i} = \frac{\partial^2 T}{\partial x_i^2}. \tag{A.15}$$

where we have dropped the $\sim$ for neatness.

In the compact form, this is denoted

$$T_t + \mathbf{u} \cdot \nabla T = \nabla^2 T$$

as in equation 2.

A.1.3 Conservation of Momentum

Finally addressing conservation of momentum, equation (A.3), we have

$$\rho \frac{Du_i}{Dt} = -\frac{\partial P}{\partial x_i} + \frac{\partial \tau_{ij}}{\partial x_j} + \rho g_i$$

(restated from above). The left side of the equation gives the inertia per volume in the fluid. Because of the creeping or low Reynolds number flow, this term is very small compared to the others. To see this, we can follow the same procedure as above to non-dimensionalize the term and compare it to the dimensionless form of the second term on the right. Using a reference density ρ_0 and the same reference velocity $u_0 = \kappa/d$ and length scale d as above, we get

$$\begin{aligned} \rho \left(\frac{Du_i}{Dt} \right) &= \rho \left(\frac{\partial u_i}{\partial t} + u_i \frac{\partial u_i}{\partial x_i} \right) \\ &= \left(\frac{\rho_0 u_0^2}{d} \right) \cdot \widetilde{\rho} \left(\frac{\partial \widetilde{u_i}}{\partial \widetilde{t}} + \widetilde{u_i} \frac{\partial \widetilde{u_i}}{\partial \widetilde{x_i}} \right). \end{aligned} \tag{A.16}$$

For comparison, we now consider the second term on the right side. We may expand the stress tensor to get

$$\frac{\partial \tau_{ij}}{\partial x_j} = \frac{\partial}{\partial x_i} \left[\eta \left(\frac{\partial u_i}{\partial x_j} + \frac{\partial u_j}{\partial x_i} - \frac{2}{3} \delta_{ij} \frac{\partial u_k}{\partial x_k} \right) \right] \tag{A.17}$$

where η is viscosity and δ_{ij} is the Kronecker delta. Introducing the characteristic reference viscosity η_0, we pull out the constants $\eta_0 u_0/d^2$ from the dimensionless form of the second term on the right side of equation A.3. Then, ignoring the other terms, we divide both sides of equation A.3 by this factor to derive as a constant on the left side of the equation

$$\begin{aligned} \frac{\rho_0 u_0^2}{d} \cdot \frac{d^2}{\eta_0 u_0} &= \frac{\rho_0 u_0 d}{\eta_0} \\ &\equiv Re_d \end{aligned} \tag{A.18}$$

where Re_d is the Reynolds number for a system with characteristic length d. Hence we see that, in our case of creeping flow ($Re_d \ll 1$), this term is relatively small. Furthermore, if we substitute $u_0 = \kappa/d$, equation (A.18) becomes

$$\begin{aligned} \frac{\rho_0 u_0 d}{\eta_0} &= \frac{\rho_0 \kappa}{\eta_0} \\ &= \frac{\kappa}{\nu} \\ &\equiv Pr^{-1} \end{aligned} \tag{A.19}$$

where $\nu \equiv \eta_0/\rho$ is the kinematic viscosity. This illustrates why the low Reynolds number approximation is often called the "infinite" (meaning sufficiently large) Prandtl number approximation. (For a rigorous proof that the limit of the Boussinesq approximation for this system is an infinite Pr, see *Wang* (2004).) In either case, we have established that the left side of the equation is sufficiently small compared to the other terms that we can assume it equals zero.

Returning to the right side of the equation, we can drop the last term of the stress tensor because $\partial u_k/\partial x_k = 0$ for incompressible flow (*Schubert et al*, 2001). Lastly, we note that, assuming we choose our coordinate system wisely, gravity need only act in one direction, so the last term is simply ρg in that direction and zero elsewhere. Thus, we are left with the simplified form of equation (A.3):

$$0 = -\frac{\partial P}{\partial x_i} + \frac{\partial}{\partial x_j}\left[\eta\left(\frac{\partial u_i}{\partial x_j} + \frac{\partial u_j}{\partial x_i}\right)\right] + \rho g_i. \tag{A.20}$$

To non-dimensionalize this equation, we first define pressure as the sum of a reference value P_0 and the deviation from that pressure, $P = P_0 + P'$. Then

$$\begin{aligned}\frac{\partial P}{\partial x_i} &= \frac{\partial}{\partial x_i}(P_0 + P') \\ &= \frac{\partial P_0}{\partial x_i} + \frac{\partial P'}{\partial x_i}\end{aligned} \tag{A.21}$$

and $\partial P_0/\partial x_i = \rho_0 g$ is the hydrostatic pressure, which is zero in all but the vertical direction. Likewise defining density as the sum of a reference density ρ_0 and the deviation from that density, $\rho = \rho_0 + \rho'$, we find that $\rho_0 g$ cancels with the hydrostatic pressure derived above, leaving $\rho' g$, which can be manipulated using thermodynamic identities:

$$\begin{aligned}\rho' g &= \overline{\left(\frac{\partial \rho}{\partial P}\right)_T} P' - \overline{\left(\frac{\partial \rho}{\partial T}\right)_P} T' \\ &= \rho_0 \overline{\chi_T} P' - \rho_0 \overline{\alpha} T'\end{aligned} \tag{A.22}$$

where $\overline{\chi_T}$ and $\overline{\alpha}$ are reference values for isothermal compressibility and thermal expansivity, respectively (*Schubert et al.*, 2001). Since we are assuming an incompressible fluid, the first of these terms is dropped. T' denotes the temperature change in the direction normal to the fluid surface.

To non-dimensionalize the middle term on the right side of equation (A.20), we introduce the quantity $\kappa/(\eta_0 d^2)$ as a characteristic pressure. Combining all the constants, we derive the non-dimensional expression

$$0 = -\frac{\partial \widetilde{P'}}{\partial \widetilde{x}_i} - \frac{\rho_0 g \overline{\alpha} \Delta T d^3}{\eta_0 \kappa} \widetilde{T}' + \frac{\partial}{\partial \widetilde{x}_i}\left[\widetilde{\eta}\left(\frac{\partial \widetilde{u}}{\partial \widetilde{x}_i} + \left\{\frac{\partial \widetilde{u}}{\partial \widetilde{x}_i}\right\}^T\right)\right]. \tag{A.23}$$

Then, as introduced in equation 4 in the body of this article, the collection of constants in the second term on the right side of this expression define the Rayleigh number, Ra:

$$Ra \equiv \frac{\rho_0 g \overline{\alpha} \Delta T d^3}{\eta_0 \kappa} \tag{A.24}$$

which, as defined in Section 2, is the dimensionless ratio of buoyant to viscous forces within the system.

Dropping the $\sim$ for neatness, equation (A.23) becomes the simplified, dimensionless equation for conservation of momentum

$$0 = -\frac{\partial P}{\partial x_i} - RaT\frac{\partial n}{\partial z} + \frac{\partial}{\partial x_j}\left[\eta\left(\frac{\partial u_i}{\partial x_j} + \frac{\partial u_j}{\partial x_i}\right)\right] + \rho g_z. \tag{A.25}$$

In the compact form, this is written

$$0 = -\nabla P + RaT\mathbf{n} + \nabla \cdot [\eta(\nabla \mathbf{u} + \{\nabla \mathbf{u}\}^T)]$$

as in equation 3.

A.2 Arrhenius Viscosity

The Arrhenius equation for temperature-dependent viscosity η an approximate law assuming a constant, homogeneous substance is

$$\eta = b \cdot \exp\left(\frac{E^* + PV^*}{RT}\right) \tag{A.26}$$

where b is a constant, E^* is the activation energy of the material, V^* is the activation volume, P is the pressure, R is the ideal gas constant, and T is the variable temperature. In this paper, we drop the PV^* term because it is relatively small compared to the activation energy E in the crust.

The Arrhenius viscosity is commonly used in rock mechanics, but without knowing outright the constant b, we get a more accurate model of viscosity by non-dimensionalizing with respect to a reference visosity, η_0. To do this, we first express the temperature as a deviation

from the surface temperature, $T = T_s + T'$, and use $\Delta T = T_b - T_s$ for the temperature scale as above, so that the exponent is re-written

$$\begin{aligned} \frac{E^*}{RT} &= \frac{E^*}{R(T_s + T')} \\ &= \frac{E^*}{R\Delta T}\frac{\Delta T}{T_s + T'} \\ &= \frac{A}{T_0 + \widetilde{T}} \end{aligned} \tag{A.27}$$

where $A = E^*/(RT)$ is a dimensionless constant, $T_0 = T_s/(T_b - T_s)$ is a non-dimensional temperature reference to surface conditions, and $\widetilde{T}$ the deviation from it. Note that $T_0 = T_s/(T_b - T_s)$ differs from the non-dimensional surface temperature $\widetilde{T}_s = (T_s - T_s)/(T_b - T_s) = 0$. The equivalent temperature reference for conditions at the bottom of the crust is

$$\begin{aligned} \frac{T_b}{T_b - T_s} &= \frac{T_b + T_s - T_s}{T_b - T_s} \\ &= \frac{T_s}{T_b - T_s} + \frac{T_b - T_s}{T_b - T_s} \\ &= T_0 + 1. \end{aligned} \tag{A.28}$$

Thus, $\widetilde{T}$ ranges from $\widetilde{T}_s = 0$ to $\widetilde{T}_b = 1$.

The reference viscosity η_0 is taken to be the viscosity at the bottom of the crust, so we will substitute $\widetilde{T} = 1$ here. We choose to use the conditions at the base of the crust for reference because this is where the temperature-dependent viscosity will be lowest, and the likelihood of convection highest. This gives

$$\begin{aligned} \widetilde{\eta} &= \frac{\eta}{\eta_0} \\ &= \frac{b \cdot \exp\left(\frac{A}{T_0 + \widetilde{T}}\right)}{b \cdot \exp\left(\frac{A}{T_0 + 1}\right)} \end{aligned} \tag{A.29}$$

from which we immediately see that the coefficients b cancel. Additionally, since the denominator is constant, we can express it simply as B_0^{-1}, leaving us with the non-dimensional Arrhenius viscosity:

$$\eta = B_0 \exp\left(\frac{A}{T_0 + \widetilde{T}}\right). \tag{A.30}$$

We note that this dimensionless expression for viscosity matches in form the dimensional version above, as desired.

This gives a dimensionless expression for the viscosity dependent only on the physical conditions summarized in ΔT and the rheological parameter E^*. However, because the Rayleigh number depends on the reference viscosity η_0, an expression for the constant b is still required. To derive b, we first return to the relationship between viscosity and the ratio of stress to strain rate,

$$\eta = \frac{\sigma}{3\dot{\epsilon}} \tag{A.31}$$

(*Ranalli*, 1995). We now use the equation for strain rate as a function of temperature (T), pressure (P), grain size (h), and shear stress (σ) introduced in equation 5 above:

$$\dot{\epsilon} = C\left(\frac{\sigma}{\mu}\right)^n \left(\frac{l}{h}\right)^m \exp\left(-\frac{E^* + PV^*}{RT}\right)$$

(*Karato and Wu*, 1993) where C is the pre-exponential factor, μ is the shear modulus, n is the stress exponent, l is the length of the Burgers vector (a description of dislocation in the crystal lattice), and m is the grain size exponent.

As in the Arrhenius viscosity, we drop the PV^* term, since it is relatively small compared to E^* in the crust, and non-dimensionalize the exponent as above. At the low stresses expected in the crust, we may assume $n = 1$, which corresponds to our assumption that flow occurs by diffusion creep only. Then, equation (A.31) above neatly returns an expression in the same form as equation(A.30), and we get that

$$b = \frac{\mu}{3C}\left(\frac{h}{l}\right)^m. \tag{A.32}$$

A.3 The Perturbation

The last equations needed for our model is a set of initial conditions that include a thermal perturbation. This will initiate convection which will either decay, remain localized, or become widespread in the model simulation. In reality, this thermal anomaly would most likely come from a mantle plume, but the source makes little difference. Following *Solomatov*, 2012, we use a simple 2D Gaussian distribution

$$T(x,z) = T_{cond}(z) + \delta T(x,z) \tag{A.33}$$

where $T_{cond}(z) = z$ is the conductive temperature profile in dimensional form and

$$\delta T(x,z) = \delta T_0 e^{-r^2} \cos(kx) \sin(\pi z) \tag{A.34}$$

is the dimensional perturbation function, δT_0 is the perturbation amplitude, k is the wavenumber of the perturbation, and r is the Euclidian distance between some origin point x_0 and the point x.

This equation is non-dimensionalized in the same way as the equations above. k and x are both scaled by the cell depth d, which cancels in the cosine term. The extra constant from the sine term and the ΔTs from scaling the temperature addends are assumed into the perturbation amplitude. The parameter r is scaled by a reference value r_0 which controls the width of the perturbed region and remains a variable in the equation. This leaves a dimensionless perturbation:

$$\tilde{T}(x,y,z) = \widetilde{z} + \delta \widetilde{T}_0 e^{-r^2/r_0^2} \cos(\widetilde{k}\tilde{x}) \sin(\pi \widetilde{z}) \tag{A.35}$$

where the $\sim$ are dropped equations 9-10 in the body of the text for simplicity.

A.4 The Critical Rayleigh Number

A numerical model programmed with the above equations will simulate convection that will either decay, remain localized, or become widespread. To get a sense of what Ra values will result in which condition before running any simulations, though, which may drastically shorten data collection time, we can independently estimate Ra_{cr} using the following model developed by *Solomatov*, 1995:

$$Ra_{cr} = Ra_{cr,n}\left[\frac{e\theta}{4(n+1)}\right]^{2(n+1)/n} \tag{A.36}$$

where $Ra_{cr,n} = {Ra_{cr,1}}^{1/n} \cdot {Ra_{cr,\inf}}^{(n-1)/n}$, $Ra_{cr,1} = 1568$, and $Ra_{cr,\inf} = 20$. Fortunately, we may continue to assume $n = 1$, which greatly simplifies the above expression to:

$$Ra_{cr} = \left(\frac{1586}{4096}e^4\right) \cdot \theta^4. \tag{A.37}$$

In this expression, θ is derived from an approximation to the Arrhenius viscosity. In place of equation (A.26) above, the exponent is approximated and simplified as follows:

$$\begin{aligned}\frac{E^*}{RT} &= \frac{E^*}{R(T_b + T')} \\ &= \frac{E^*}{RT_b(1 + \frac{T'}{T_b})} \\ &= \frac{E^*}{RT_b}\left(1 - \frac{T'}{T_b}\right) \\ &= \frac{E^*}{RT_b} - \frac{E^*T'}{RT_b^2}\end{aligned} \tag{A.38}$$

where the third equality follows approximately from Taylor expansion. Now, since we are examining an exponent and the first term after the last equality is a constant, this term can be removed from the exponent, and the remainder written as a function of non-dimensional temperature:

$$\begin{aligned}\frac{E^*}{RT} &\sim -\frac{E^* T'}{RT_b^2} \\ &= -\left(\frac{E^* \Delta T}{RT_b^2}\right)\frac{T'}{\Delta T} \\ &= -\theta \widetilde{T}'\end{aligned} \tag{A.39}$$

and so

$$\theta = \frac{E^* \Delta T}{RT_b^2}. \tag{A.40}$$

Here, temperature is expressed as a deviation from the temperature at the bottom of the crust T_b instead of a deviation from the surface temperature T_s to account for the reference viscosity being that at the bottom of the crust. Before, we were able to use T_s instead (which is more intuitive because it is both the lowest temperature and non-variant, unlike T_b) because the reference depth was determined by the parameter $\widetilde{T}$, which varied from 0 at the surface to 1 at the bottom of the crust. However, in this simplified model for viscosity, the parameter θ controls all aspects of the model, including the reference depth, so it is important that T_b is used here.

This gives an equation for an estimate Ra_{cr}

$$Ra_{cr} = \left(\frac{1586}{4096}e^4\right) \cdot \left(\frac{E^* \Delta T}{RT_b^2}\right)^4. \tag{A.41}$$

References

Alikina, O. N., and E. L. Tarunin (2000), Subcritical motions of a fluid with temperature-dependent viscosity, *Fluid Dyn.*, *36*, 574-580.

Anderson, F. S., and S. E. Smrekar (2006), Global mapping of crustal and lithospheric thickness on Venus, *J. Geophys. Res.*, *111*, E08006, doi:10.1029/2004JE002395.

Barr, A. C., and R. R. Pappalardo (2005), Onset of convection in the icy Galilean satellites: Influence of rheology, *Geophys. Res. Lett.*, *110*, doi:10.1029/2004JE0002371.

Barr, A. C., and W. B. McKinnon (2007), Convection in Enceladus' ice shell: Conditions for initiation *Geophys. Res. Lett.*, *34*, doi:10.1029/2006GL028799.

Bercovici, D. (2003), The generation of plate tectonics from mantle convection, *Earth Planet. Sci. Lett.*, *205*, 107-121.

Bottaro, A., P. Metzener, and M. Matalon (1992), Onset and two-dimensional patterns of convection with strongly temperature-dependent viscosity, *Phys. Fluids*, *4*, 655-663.

Busse, F. H. (1967), The stability of the finite amplitude cellular convection and its relation to an extremum principle, *J. Fluid Mech*, *30*, 625-649.

Capone, F., and M. Gentile (1994), Nonlinear stability analysis of convection for fluids with exponentially temperature-dependent viscosity, *Acta Mech.*, *107*, 53-64.

Courtillot, V., A. Davaille, J. Besse, and J. Stock (2003), Three distinct types of hotspots in the Earth's mantle, *Earth Planet. Sci. Lett.*, *205*, 295-308.

Dawes, J. H. P. (2010), The emergence of a coherent structure for coherent structures: Localized states in nonlinear systems, *Phil. Trans. R. Soc.*, *A 368*, 3519-3534.

Dombard, A. J., C. L. Johnson, M. A. Richards, and S. C. Solomon (2007), A magmatic loading model for coronae on Venus, *J. Geophys. Res.*, *112*, E04006, doi:10.1029/2006JE002731.

Fowler, A. C. (1993), Boundary layer theory and subduction, *J. Geophys. Res. 98*, 21,997-22,995.

Grindrod, P. M., and T. Hoogenboom (2006), Venus: The corona conundrum, *Astron. Geophys.*, *47*(3), 16-21.

Hansen, V. L. (2003), Venus diapirs: Thermal or compositional?, *Geol. Soc. Am. Bull.*, *115*, 1040-1052.

Harder, H. and U. R. Christensen (1996), A one-plume model of Martian mantle, *Nature*, *380*, 507-509.

Head, J. W., L. S. Crumpler, J. C. Aubele, J. Guest, and S. R. Saunders (1992), Venus volcanism: Classification of volcanic features and structures, associations, and global distribution from Magellan data, *J. Geophys. Res.*, *97*, 13,153-13,197.

Hirth, G., and D. Kohlstedt (2003), Rheology of the upper mantle and the mantle wedge: A view from the experimentalists, in *Inside the Subduction Factory*, edited by J. Eiler, pp. 83-105, AGU, Washington, D.C.

Janes, D. M., S. W. Squyres, D. L. Bindschadler, G. Baer, G. Schubert, V. L. Sharpton, and H. E. Stofan (1992), Geophysical models for the formation and evolution of coronae on Venus, *J. Geophys. Res.*, *97*(16), 16,055-13,634.

Johnson, C. L., and M. A. Richards (2003), A conceptual model for the relationship between coronae and large-scale mantle dynamics on Venus, *J. Geophys. Res.*, *108*, doi:10.1029/2002JE001962.

Karato, S.-I., M. S. Paterson, and J. D. FitzGerald (1986), Rheology of synthetic olivine aggregates: Influence of grain size and water, *J. Geophys. Res.*, *91*, 8151-8176.

Karato, S.-I., and P. Wu (1993), Rheology of the upper mantle: A synthesis, *Science*, *260*, 771-778.

Ke, Y. and V. S. Solomatov (2006), Early transient superplumes and the origin of the Martian crustal dichotomy, *J. Geophys. Res.*, *111*, doi: 10.1029/2005JE002631.

King, S. D. (2008), Pattern of lobate scarps on Mercury's surface reproduced by a model of mantle convection, *Nat. Geosci.*, *1*, 229-232.

Koch, D. M., and M. Manga (1996), Neutral buoyant diapirs: A model for Venus coronae, *Geophys. Res. Lett.*, *99*, 225-228.

Korenaga, J., and S.-I. Karato (2008), A new analysis of experimental data on olivine rheology, *J. Geophys. Res.*, *113*, B02403, doi:10.1029/2007JB0055100.

Korenaga, J. (2010), On the likelihood of plate tectonics on super-Earths: Does size matter?, *Astrophys. J.*, *725*, L43-L46.

Kucinskas, A. B., and D. L. Turcotte (1994), Isostatic compensation of the equatorial highlands on Venus, *Icarus*, *112*, 104-116.

Mackwell, S.J., M. E. Zimmerman, and D. L. Kohlstedt (1998), High-temperature deformation of dry diabase with application to tectonics of Venus, *J. Geophys. Res.*, *103*, 975-984.

McKenzie, D. P. (1994), The relationship between topography and gravity on Earth and Venus, *Icarus*, *112*, 55-58.

McKinnon, W. B. (1999), Convective instability in Europa's floating ice shell, *Geophys. Res. Lett.*, *26*, 951-954.

Mitri, G., and A. P. Showman (2008), Thermal convection in ice-I shells of Titan and Enceladus, *Icarus*, *139*, 387-396.

Moore, W. B., and G. Schubert (1997), Venusian crustal and lithospheric properties from non-linear regressions of highland geoid and topography, *Icarus*, *128*, 412-428.

Moresi, L.-N., and V. S. Solomatov (1995), Numerical investigation of 2D convection with extremely large viscosity variations, *Phys. Fluids*, *7*, 2154-2162.

Moresi, L.-N., and V. S. Solomatov (1998), Mantle convection with a brittle lithosphere: Thoughts on the global tectonic style of the Earth and Venus, *Geophys. J.*, *133*, 669-682.

Mueller, N., J. Helbert, G. L. Hashimoto, C. C. C. Tsang, S. Erard, G. Piccioni, and P. Drossart (2008), Venus surface thermal emission at 1 μm in VIRTIS imaging observations: Evidence for variation of crust and mantle differentiation conditions, *J. Geophys. Res.*, *113*, E00B17, doi:10.1029/2008JE003118.

Nimmo, R., and D. McKenzie (1996), Modelling plume related uplift, gravity and melting on Venus, *Earth Planet. Sci. Lett.*, *145*, 109-123.

Nimmo, F., and D. McKenzie (1998), Volcanism and tectonism on Venus, *Annu. Rev. Earth Planet. Sci.*, *26*, 23-51.

O'Neill, C., A. M. Jellinek, and A. Lenardic (2007), Conditions for the onset of plate tectonics on terrestrial planets and moons, *Earth Planet. Sci. Lett.*, *261*, 20-32.

Orth, C., and V. S. Solomatov (2009), The effects of dynamic support and thermal isostasy on the topography and geoid of Venus, Abstract 1811 presented at 40^th Lunar Planet. Sci. Conf., The Woodlands, Texas, 23-27 Mar.

Orth, C., and V. S. Solomatov (2012), Constraints on the Venusian crustal thickness variations in the isostatic stagnant lid approximation, *Geochem. Geophys. Geosyst.*, *13*, Q11012, doi:10.1029/2012GC004377.

Phillips, R. J. (1994), Estimating lithospheric properties at Atla Regio Venus, *Icarus*, *112*, 147-170.

Purwins, H.-G., H. U. Bödeker, and Sh. Amiranashvili (2010), Dissipative solitons, *Adv. Phys.*, *59*, 485-701.

Ranalli, G. (1995), *Rheology of the Earth*, Chapman & Hall, London.

Redmond, H. L., and S. D. King (2007), Does mantle convection currently exist on Mercury?, *Phys. Earth Planet. Inter.*, *164*, 221-231.

Reese, C. C., C. P. Orth, and V. S. Solomatov (2011), Impact megadomes and the origin of the Martian crustal dichotomy, *Icarus*, *213*, 433-442.

Reese, C. C., V. S. Solomatov, and C. P. Orth (2007), Mechanisms for cessation of magmatic resurfacing on Venus, *J. Geophys. Res.*, *112*, E04S04, doi:10.1029/2006JE002782.

Reese, C. C., V. S. Solomatov, J. R. Baumgardner, and D. R. Stegman (2004), Magmatic evolution of impact-induced Martial mantle plumes and the origin of Tharsis, *J. Geo. Res.*, *109*, E08009, doi: :10.1029/2003JE002222.

Richter, F. M., H. C. Nataf, and S. Daly (1983), Heat transfer and horizontally averaged temperature of convection with large viscosity variations, *J. Fluid. Mech.*, *129*, 173-192.

Roberts, J. H., and Barnouin, O. S. (2012), The effect of the Caloris impact on the mantle dynamics and volcanism of Mercury, *J. Geophys. Res.*, *117*, E02007, doi: 10.1029/2011JE003876.

Rybacki, E., and G. Dresen (2000), Dislocation and diffusion creep of synthetic anorthite aggregates, *J. Geophys. Res.*, *105*, 26,017-26,036.

Sandwell, D., and G. Schubert (1995), A global survey of possible subduction sites on Venus, *Icarus*, *117*, 173-196.

Schubert, G., D. L. Turcotte, and P. Olson (2001), *Mantle Convection in the Earth and Planets*, Cambridge Univ. Press, New York.

Segel, L. A., and J. T. Stuart (1962), On the question of the preferred mode in cellular thermal convection, *J. Fluid Mech*, *13*, 289-306.

Shelton, G., and J. Tullis (1981), Experimental flow laws for crustal rocks (abstract), *Eos. Trans. AGU*, *62*, 396.

Simons, M., S. C. Solomon, and B. H. Hager (1997), Localization of gravity and topography: Constraints on the tectonics and mantle dynamics of Venus, *Geophys. J. Int.*, *131*, 24-44.

Smrekar, S. E., E. R. Stofan, N. Mueller, A. Treiman, L. ElkinsTanton, J. Helbert, G. Piccioni, and P. Drossart (2010), Recent hotspot volcanism on Venus from VIRTIS emissivity data, *Science*, *328*(5978), 605-608.

Smrekar, S. E. (1994), Evidence for active hotspots on Venus from analysis of Magellan gravity data, *Icarus*, *112*, 2-26.

Solomatov, V. S., and A. C. Barr (2006), Onset of convection in fluids with strongly temperature-dependent, power-law viscosity, *Phys. Earth Planet. Sci*, *155*, 140-145.

Solomatov, V. S., and A. C. Barr (2008), Onset of convection in fluids with strongly temperature-dependent, power-law viscosity: 2, *Phys. Earth Planet. Sci*, *165*, 1-13.

Solomatov, V. S., and C. C. Reese (2008), Grain size variations in the Earth's mantle and the evolutions of primordial chemical heterogeneities, *J. Geophys. Res.*, *113*, B07408, doi: 10.1029/2007JB005319.

Solomatov, V. S., and L.-N. Moresi (1996), Stagnant lid convection on Venus, *J. Geophys. Res.*, *101*, 4737-4753.

Solomatov, V. S. (1995), Scaling of temperature- and stress-dependent viscosity convection, *Phys. Fluids*, *7*, 266-274.

Solomatov, V. S. (2012), Localized subcritical convective cells in temperature-dependent viscosity fluids, *Phys. Earth Planet. Int.*, *200-201*, 63-71.

Squyres, S. W., D. M. Janes, G. Baer, D. L. Bindschadler, G. Schubert, V. L. Sharpton, and E. R. Stofan (1992), The morphology and evolution of coronae on Venus, *J. Geophys. Res.*, *97*, 13,611-13,634.

Stegman, D. R., A. M. Jellinek, S. A. Zatman, J. R. Baumgardner, and M. A. Richards (2003), An early lunar core dynamo driven by thermochemical mantle convection, *Nature*, *421*, 143-146.

Stengel, K. C., D. C. Oliver, and J. R. Booker (1982), Onset of convection in a variable viscosity fluid, *J. Fluid. Mech.*, *120*, 441-431.

Stofan, E. R., V. E. Hamilton, D. M. Janes, and S. E. Smrekar (1997), Coronae on Venus: Morphology and origin, In S. W. Bougher, D. M. Hunten, R. J. Phillips (Eds.), *Venus II: Geology, Geophysics, Atmosphere, and Solar Wind Environment*, Univ. Arizona Press, Tuscon, 931-966.

Stofan, E. R., V. L. Sharpton, G. Schubert, G. Baer, D. L. Bindschadler, D. M. James, and S. W. Squyres (1992), Global distribution and characteristics of coronae and related features on Venus: Implication for origin and relation to mantle processes, *J. Geophys. Res.*, *97*, 13,347-13,378.

Surkov, Y. A., L. P. Moskalyeva, P. P. Schcheglov, V. P. Karyukova, O.S. Manvelyan, V. S. Kirichenko, and A. D. Dudin (1983), Determination of the elemental composition of rocks on Venus by Venera 13 and 14, *Proc. Lunar Planet. Sci. Conf. 13th, Part 2*, *J. Geophys. Res.*, *88*, A481-A493.

Surkov, Y. A., L. P. Moskalyeva, V. P. Kharyukova, A. D. Dudin, G. G. Smirnov, and S. Y. Zaitseva (1986), Venus rock composition at the Vega 2 landing site, *Proc. Lunar Planet. Sci. Conf. 17th, Part 1*, *J. Geophys. Res.*, *91*, E215-E218.

Surkov, Y. A., V. L. Varsukov, L. P. Moskalyeva, V. P. Kharyukova, and A. L. Kemurdzhian (1984), New data on the composition, structure and properties of Venus rock obtained by Venera 13 and 14, *Proc. Lunar Planet. Sci. Conf. 14^{t}h, Part 1*, *J. Geophys. Res.*, *89*, B393-B402.

Thual, O., and S. Fauve (1988), Localized structures generated by subcritical instabilities, *J. Phys. France*, *49*, 1829-1833.

Trompert, R., and U. Hansen (1998), Mantle convection simulations with rheologies that generate plate-like behaviour, *Nature*, *395*, 686-689.

Turcotte, D. L. (1993), An episodic hypothesis for Venusian tectonics, *J. Geophys. Res.*, *98*, 17,061-17,068.

Valencia, D., R. J. OConnell, and D. D. Sasselov (2007), Inevitability of plate tectonics on super-Earths, *Astrophys. J.*, *670*, L45-L48.

van Heck, H. J., and P. J. Tackley (2011), Plate tectonics on super-Earths: Equally or more likely than on Earth, *Earth Planet. Sci. Lett.*, *310*, 252-261.

van Saarloos, W., and P. C. Hohenberg (1992), Fronts, pulses, sources and sinks in generalized complex Ginzburg-Landau equations, *Physica D*, *56*, 303-367.

Vezolainen, A. V., V. S. Solomatov, A. T. Basilevsky, and J. W. Head (2004), Uplift of Beta Regio: Three-dimensional models, *J. Geophys. Res.*, *109*, E08007, doi:10.1029/2004JE002259.

Vezolainen, A. V., V. S. Solomatov, J. W. Head, A. T. Basilevsky, and L.-N. Moresi (2003), Timing of formation of Beta Regio and its geodynamical implications, *J. Geophys. Res.*, *108*(E1), 5002, doi:10.1029/2002JE001889.

Wang, X. (2004), Infinite Prandtl number limit of Rayleigh-Bérnard convection, *Comm. Pure App. Math.*, *57*, 1265-1285.

Wenzel, M. J., M. Manga, and A. M. Jellinek (2004), Tharsis as a consequence of Mars' dichotomy and layered mantle, *Geophys. Res. Lett.*, *31*, L04702, doi: 10.1029/2003GL019306.

White, D. B. (1988), The planforms and onset of convection with a temperature-dependent viscosity, *J. Fluid Mech*, *191*, 247-286.

Zhong, S. J., and M. T. Zuber (2001), Degree-1 mantle convection and the crustal dichotomy on Mars, *Earth Planet. Sci. Lett.*, *189*, 75-84.

Zhong, S. (2008), Migration of Tharsis volcanism on Mars caused by differential rotation of the lithosphere, *Nat. Geosci*, *2*, 19-23.